

Reduced-Model Based Fault Detector and Controller Design for Discrete-Time Switching Fuzzy Systems

Yaoyao Tan, Xiaojie Su, Zhenshan Bing, Xiaokui Yang, and Alois Knoll

Abstract—The reduced model-based coordinated design of fault detectors and controllers for discrete-time switching fuzzy systems is examined. First, the mean-square exponential stabilization of switching Takagi-Sugeno fuzzy systems is performed using the average dwell time method under an arbitrary switching law. Next, using segmented Lyapunov function techniques, a dynamic full- and reduced-order fault detector and controller is designed to ensure that the overall dynamic residual system is mean-square exponentially stable with a balanced \mathcal{H}_∞ performance level (ξ, β) . The solvability conditions for the fault detector and controller are derived using a linearization method, and the relevant parameters can be determined using the mathematical linear matrix solver toolbox. Two examples including a switching Chua's circuit system are presented to demonstrate the effectiveness of the proposed fault detector and controller.

Index Terms—Fuzzy systems, fault detection, fuzzy control, switched systems

I. Introduction

A broad class of engineering systems and processes, including physical experimental systems, advanced traffic control systems, and automated vehicle high-speed systems, can be described as hybrid switching systems [1], which consist of a limited number of subsystems and a switching law that determines the active subsystem at an arbitrary or expected moment [2], [3]. In addition, a series of intelligent control techniques based on hybrid switch controllers have been developed [4], which can effectively overcome the limitations of traditional single controllers and enhance the performance of closed-loop systems [5]. According to the relevant analyses, research on switching systems is of significance for the following two reasons [6], [7]: 1) Owing to their intrinsic switching characteristics, many practical engineering systems can be modeled as switching systems; 2) in several cases, the performance of a controller in achieving the control goal is not satisfactory, and thus, multiple controllers must be adopted.

This work was supported by the Key-Area Research and Development Program of Guangdong Province under Grant (2020B0909020001), the National Natural Science Foundation of China (62173051), the Graduate Research and Innovation Foundation of Chongqing, China (CYB21064), and Chongqing Science Fund for Outstanding Young Scholars (cstc2019jcyjqqX0015). Corresponding author: Xiaojie Su.

Y. Tan, and X. Su are with the College of Automation, Chongqing University, China. Email: tanyaoyao@cqu.edu.cn; suxiaojie@cqu.edu.cn.

Z. Bing and A. Knoll are with the Department of Informatics Technical University of Munich, Germany. Email: bing@in.tum.de; knoll@in.tum.de

X. Yang is with the Southwest Technology and Engineering Research Institute, Chongqing 400039, China. Email: swsc10@yeah.net

A key approach to design nonlinear control systems is to use a Takagi-Sugeno (T-S) fuzzy method [8] to approximately express dynamic nonlinear systems. This model represents intelligent control methods that imitate human empirical reasoning and decision-making processes [9]. The T-S fuzzy model is expressed by a set of regular or empirical rules, which establishes the local linear input-output relations of a dynamic nonlinear discrete- or continuous-time system [10]. [11]–[14] introduce the fuzzy modeling process in detail, and the latter three articles also describe the process of designing a fuzzy state feedback controller. As a matter of fact, the fuzzy control technology can be applied to many engineering projects, such as behavior-based robot control [15], automobile servo control [16], intelligent traffic control [17] and so on.

The modeling and control of switching system based on fuzzy control technology has received much attention of many researchers. For the prospect of practical engineering application, the switching fuzzy system, as a new kind of dynamic composite system, is worthy to be focused by more scholars. So far, many articles related to the modeling and control of switching fuzzy systems have been published: dynamic output feedback controller in [18], fault-tolerant control in [19], asynchronous \mathcal{H}_∞ filter in [20], observer in [21], antidisturbance control in [22], state feedback controller in [23]–[25], etc. Obviously, the discretization process exists in most practical engineering systems [26], and the number of existing studies on discrete-time switching systems is considerably less than that on continuous-time switching systems. Moreover, for systems that are inconvenient to measure the state variables directly, the state feedback controller can not be widely used in the actual systems [27]. In addition, research on discrete-time switching T-S fuzzy systems considering stochastic uncertainties remains limited. Because stochastic uncertainties [28] frequently appear in practical engineering systems, it is necessary to extensively examine systems with stochastic uncertainties.

During system operation, owing to the harsh environment and other nonhuman factors, the sensors or actuators in the system will may incur damage [29] or undergo failures, resulting in irreparable damage to the system [30]. Therefore, the system fault detection and fault-tolerant control must be robust to prevent accidents and ensure safe and smooth production [31]. Although certain researchers have focus on this aspect [32]–[35], research on fault detection and fault-tolerant control of switching T-S

fuzzy stochastic systems is limited owing to the complexity of switching systems. Specifically, due to the particularity of switching system, the fault detection of this kind of system needs to be paid more attention [36].

To sum up, this paper has following three starting points: 1) For systems with switching characteristics in practical applications, it is necessary to study T-S fuzzy technology for local linearization to approximate the original nonlinear switching system; 2) If there exist stochastic uncertainties in the original system, the probability of system failure increases. In order to solve these practical problems, the collaborative design of fault detector and controller is needed; 3) For the sake of reducing the computational complexity of high-order system and ensuring the real-time performance of calculation, the order reduction technology for high-order system is worth studying. Therefore, this paper presents the design of a full- and reduced-order fault detector and controller (FRFDC) for discrete-time switching systems with stochastic uncertainties. The dynamic switching subsystems are described by fuzzy variables instead of a single numerical value. The main contributions of this paper can be summarized as follows:

- 1) A class of discrete-time switching fuzzy systems with noise disturbances, stochastic uncertainties and fault signals are studied, and then a cooperative design strategy of fuzzy fault detector and controller is proposed.
- 2) The reduced-order fault detector and controller are designed by using the model reduction technology, which reduces the computational complexity on the basis of ensuring the residual system performance.
- 3) Based on the proposed theoretical method, the effectiveness and feasibility of the proposed method are verified by modeling and analyzing the switching Chua's circuit system.

II. System Description and Preliminaries

Based on the motivations of this paper, we consider a class of discrete-time switching systems with noise disturbances, stochastic uncertainties and fault signals, and then use fuzzy control technology to conduct fuzzy modeling for all switching subsystems. The plant model is established as follows:

Plant Form:

Rule $\mathcal{H}_i^{[s]}$: IF $\sigma_1^{[s]}(k)$ is $\varrho_{i1}^{[s]}$ and $\sigma_2^{[s]}(k)$ is $\varrho_{i2}^{[s]}$ and ... and $\sigma_\tau^{[s]}(k)$ is $\varrho_{i\tau}^{[s]}$, THEN

$$x(k+1) = A_i^{[s]}x(k) + B_i^{[s]}u(k) + D_{1i}^{[s]}d(k) + D_{2i}^{[s]}x(k)\omega(k) + E_i^{[s]}(h)f(k) \quad (1a)$$

$$y(k) = C_i^{[s]}x(k) + L_i^{[s]}d(k) + F_i^{[s]}f(k) \quad (1b)$$

where $x(k) \in \mathbb{R}^m$ is the state vector; $y(k) \in \mathbb{R}^n$ is the measurement output; $d(k) \in \mathbb{R}^p$ is the noise vector belonging to $\ell_2[0, \infty)$; $f(k) \in \mathbb{R}^q$ is the fault signal belonging to $\ell_2[0, \infty)$; $\omega(k)$ is the scalar stochastic uncertainty defined on the probability space $(\Omega, \mathcal{F}, \mathcal{P})$ relating to an increasing family $(\mathcal{F}_k)_{k \in \mathbb{N}}$ of σ -algebras $\mathcal{F}_k \subset \mathcal{F}$ generated by

$(\omega(k))_{k \in \mathbb{N}}$, which is independent and satisfies $\mathbb{E}\{\omega(k)\} = 0$ and $\mathbb{E}\{\omega^2(k)\} = \eta$. r is the number of fuzzy rules. $\{\varrho_{i1}^{[s]}, \dots, \varrho_{i\tau}^{[s]}\}$ is the fuzzy set. $\{\sigma_1^{[s]}(k), \sigma_2^{[s]}(k), \dots, \sigma_\tau^{[s]}(k)\}$ is the premise variable set. \mathcal{N} is a positive scalar, which represents the number of switching subsystems.

$$\rho_s(k) : [0, \infty) \rightarrow \{0, 1\}$$

is a set of switching sequences, which decides to boot a subsystem at a certain instant and satisfies

$$\rho_1(k) + \rho_2(k) + \dots + \rho_s(k) = 1, \quad s \in 1, 2, \dots, \mathcal{N}$$

$A_i^{[s]}$ is a real constant matrix of the switching T-S fuzzy system, and $B_i^{[s]}$, $D_{1i}^{[s]}$, $D_{2i}^{[s]}$, $E_i^{[s]}$, $C_i^{[s]}$, $L_i^{[s]}$, and $F_i^{[s]}$ are defined in the same way as $A_i^{[s]}$.

Suppose that the control input $u(k)$ and premise variables $\sigma^{[s]}(k)$ are independent of each other. The original switching T-S fuzzy system can be rewritten as

Rule $\mathcal{H}_i^{[s]}$: IF $\sigma_1^{[s]}(k)$ is $\varrho_{i1}^{[s]}$ and $\sigma_2^{[s]}(k)$ is $\varrho_{i2}^{[s]}$ and ... and $\sigma_\tau^{[s]}(k)$ is $\varrho_{i\tau}^{[s]}$, THEN

$$x(k+1) = A_i^{[s]}x(k) + B_i^{[s]}u(k) + D_{1i}^{[s]}d(k) + D_{2i}^{[s]}x(k)\omega(k) + E_i^{[s]}(k)f(k) \quad (2a)$$

$$y(k) = C_i^{[s]}x(k) + L_i^{[s]}d(k) + F_i^{[s]}f(k) \quad (2b)$$

where

$$A_i^{[s]}(k) \triangleq \sum_{s=1}^{\mathcal{N}} \rho_s(k) \sum_{i=1}^r h_i^{[s]}(\sigma^{[s]}(k)) A_i^{[s]}$$

and $B_i^{[s]}(k)$, $D_{1i}^{[s]}(k)$, $D_{2i}^{[s]}(k)$, $E_i^{[s]}(k)$, $C_i^{[s]}(k)$, $L_i^{[s]}(k)$ and $F_i^{[s]}(k)$ are defined in the same way as $A_i^{[s]}(k)$. In addition, the fuzzy basis functions are defined as follows

$$h_i^{[s]}(\sigma^{[s]}(k)) \triangleq \frac{\theta_i^{[s]}(\sigma^{[s]}(k))}{\sum_{i=1}^r \theta_i^{[s]}(\sigma^{[s]}(k))}, \quad \sum_{i=1}^r h_i^{[s]}(\sigma^{[s]}(k)) = 1$$

$$h_i^{[s]}(\sigma^{[s]}(k)) \geq 0, \quad \theta_i^{[s]}(\sigma^{[s]}(k)) \geq 0$$

where

$$\theta_i^{[s]}(\sigma^{[s]}(k)) \triangleq \left\{ \varrho_{i1}^{[s]}(\sigma_1^{[s]}(k)) \right\} \times \left\{ \varrho_{i2}^{[s]}(\sigma_2^{[s]}(k)) \right\} \times \dots \times \left\{ \varrho_{i\tau}^{[s]}(\sigma_\tau^{[s]}(k)) \right\}$$

Remark 1. Stochastic uncertainty $\omega(k)$ is considered a type of multiplicative noise in this switching T-S fuzzy system, which is irregular and bounded in a small period. In a large period, the sequence $\omega(k)$ represent a set of points that conform to a certain rule. In our work, $\omega(k)$ is a one-dimensional set of zero-mean Gaussian white noise sequences, that is, $\mathbb{E}\{\omega(k)\} = 0$ and $\mathbb{E}\{\omega^2(k)\} = \eta$.

Suppose that rule sets $\mathcal{H}_i^{[s]}$ are available for the fault detector and controller design. To achieve fault detection, the structure of the dynamic fuzzy controller model is established as follows:

Fault Detector and Controller Form:

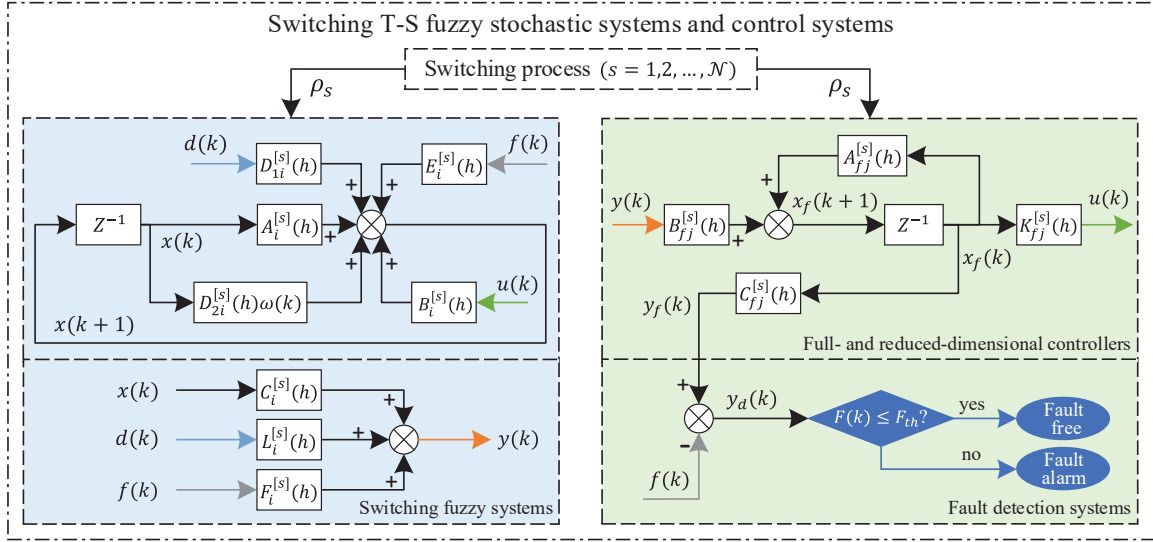


Fig. 1. Block diagram of the overall dynamic residual system

Rule $\mathcal{H}_j^{[s]}$: IF $\sigma_1^{[s]}(k)$ is $\varrho_{j1}^{[s]}$ and $\sigma_2^{[s]}(k)$ is $\varrho_{j2}^{[s]}$ and ... and $\sigma_r^{[s]}(k)$ is $\varrho_{jr}^{[s]}$, THEN

$$x_f(k+1) = A_{fj}^{[s]}(k)x_f(k) + B_{fj}^{[s]}(k)y(k) \quad (3a)$$

$$u(k) = K_{fj}^{[s]}(k)x_f(k) \quad (3b)$$

$$y_f(k) = C_{fj}^{[s]}(k)x_f(k) \quad (3c)$$

$$y_d(k) = y_f(k) - f(k) \quad (3d)$$

where $x_f(k) \in \mathbb{R}^f$ is the state vector, and $A_{fj}^{[s]}(k)$, $B_{fj}^{[s]}(k)$, $C_{fj}^{[s]}(k)$ and $K_{fj}^{[s]}(k)$ are defined in the same way as equation (2), which are all designed later with full- and reduced-dimensions.

Then, the overall dynamic residual system can be given as

$$\begin{aligned} \bar{x}(k+1) &= \sum_{s=1}^N \rho_s(k) \sum_{i=1}^r h_i^{[s]}(\sigma^{[s]}(k)) \sum_{j=1}^r h_j^{[s]}(\sigma^{[s]}(k)) \\ &\quad \times \left[\bar{A}_{ij}^{[s]} \bar{x}(k) + \bar{D}_{ij}^{[s]} \varpi(k) + \bar{D}_{2i}^{[s]} x(k) \omega(k) \right] \end{aligned} \quad (4a)$$

$$\begin{aligned} y_d(k) &= \sum_{s=1}^N \rho_s(k) \sum_{i=1}^r h_i^{[s]}(\sigma^{[s]}(k)) \sum_{j=1}^r h_j^{[s]}(\sigma^{[s]}(k)) \\ &\quad \times \left[\bar{C}_j^{[s]} \bar{x}(k) + \bar{F}_0^{[s]} \varpi(k) \right] \end{aligned} \quad (4b)$$

where

$$\bar{x}(k) \triangleq \begin{bmatrix} x(k) & x_f(k) \end{bmatrix}^T, \quad \varpi(k) \triangleq \begin{bmatrix} d(k) & f(k) \end{bmatrix}^T$$

and

$$\begin{aligned} \bar{A}_{ij}^{[s]} &\triangleq \begin{bmatrix} A_i^{[s]} & B_i^{[s]} K_{fj}^{[s]} \\ B_{fj}^{[s]} C_i^{[s]} & A_{fj}^{[s]} \end{bmatrix}, \quad \bar{C}_j^{[s]} \triangleq \begin{bmatrix} 0_{1 \times n} & C_{fj}^{[s]} \end{bmatrix} \\ \bar{D}_{ij}^{[s]} &\triangleq \begin{bmatrix} D_{1i}^{[s]} & E_i^{[s]} \\ B_{fj}^{[s]} L_i^{[s]} & B_{fj}^{[s]} F_i^{[s]} \end{bmatrix}, \quad \bar{D}_{2i}^{[s]} \triangleq \begin{bmatrix} D_{2i}^{[s]} & 0_{n \times n} \\ 0_{n \times n} & 0_{n \times n} \end{bmatrix} \\ \bar{F}_0^{[s]} &\triangleq \begin{bmatrix} 0_{1 \times 1} & -I_{1 \times 1} \end{bmatrix} \end{aligned}$$

The block diagram of the overall dynamic residual system (4) is shown in Fig. 1. Then, the following two definitions are introduced for subsequent derivations.

Definition 1. [37] For any $\chi \in [1, \infty)$ and $\vartheta \in [0, 1]$, supposing we have $\mathbb{E}\{\|\bar{x}(k)\|\} \leq \chi \|\bar{x}(k_0)\| \vartheta^{k-k_0}$, for all $k \geq k_0$, then the dynamic residual system satisfies mean-square exponentially stable (MSES) under a set of random switching rules.

Definition 2. [37] For any $\xi \in (0, \infty)$ and $\beta \in (0, 1)$, the dynamic residual system is guaranteed to has an \mathcal{H}_∞ performance level (ξ, β) if it stabilizes in mean-square exponential way when $\varpi(k) \equiv 0$, and under the initial condition of $\bar{x}(k) = 0$, for all nonzero $\varpi(k) \in \ell_2[0, \infty)$, the following inequality holds:

$$\mathbb{E} \left\{ \sum_{s=k_0}^{\infty} \beta^s y_d^T(s) y_d(s) \right\} < \xi^2 \mathbb{E} \left\{ \sum_{s=k_0}^{\infty} \varpi^T(s) \varpi(s) \right\} \quad (5)$$

To formulate the fault detection problem, a residual evaluation function $F(y_d)$ is constructed to evaluate the residual signal. Define

$$F(y_d) \triangleq \mathbb{E} \left\{ \left[\sum_{\varsigma=0}^k y_d^T(\varsigma) y_d(\varsigma) \right]^{\frac{1}{2}} \right\} \quad (6)$$

The fault signal can be detected by selecting a threshold

$$F_{th} \triangleq \sup_{0 \neq \varpi \in \ell_2, f=0} F(y_d) \quad (7)$$

Then, the relationship between F_{th} and $F(y_d)$ is shown as follows

- 1) $F(y_d) > F_{th}$: fault threshold valve is triggered;
- 2) $F(y_d) \leq F_{th}$: fault threshold valve is not triggered.

III. System Performance Analysis

This section will analyze the stability of the overall dynamic residual system (4) to obtain the sufficient conditions for the design of FRFDC.

Theorem 1. Given scalars $\xi > 0$, $0 < \beta < 1$ and $\varepsilon \geq 1$, supposing there exist positive definite symmetric matrix $P^{[s]}$, such that the following inequalities hold for $l, s \in \mathcal{N}$

$$\Omega_{ii}^{[s]} < 0, \quad i = 1, 2, \dots, r \quad (8a)$$

$$\frac{1}{r-1} \Omega_{ii}^{[s]} + \frac{1}{2} (\Omega_{ij}^{[s]} + \Omega_{ji}^{[s]}) < 0, \quad 1 \leq i < j \leq r \quad (8b)$$

$$P^{[s]} - \varepsilon P^{[l]} \leq 0, \quad \forall s, l \in \mathcal{N} \quad (8c)$$

where

$$\begin{aligned} \Omega_{ij}^{[s]} &\triangleq \begin{bmatrix} \Upsilon_{110}^{[s]} & \Upsilon_{2ij}^{[s]} \\ \star & \Upsilon_{330}^{[s]} \end{bmatrix}, \quad \Upsilon_{110}^{[s]} \triangleq \begin{bmatrix} -\beta P^{[s]} & 0 \\ 0 & -\xi^2 I \end{bmatrix} \\ \Upsilon_{2ij}^{[s]} &\triangleq \begin{bmatrix} (\bar{A}_{ij}^{[s]})^T & (\bar{C}_j^{[s]})^T & (\bar{D}_{2i}^{[s]})^T \\ (\bar{D}_{ij}^{[s]})^T & (\bar{F}_0^{[s]})^T & 0 \end{bmatrix} \\ \Upsilon_{330}^{[s]} &\triangleq \begin{bmatrix} -(P^{[s]})^{-1} & 0 & 0 \\ 0 & -I & 0 \\ 0 & 0 & -(\eta P^{[s]})^{-1} \end{bmatrix} \end{aligned}$$

then, for a series of arbitrary switching signals with the average dwell time $T_a > T_a^* = \frac{\ln \varepsilon}{\beta}$, the overall dynamic residual system (4) is MSES with a balanced \mathcal{H}_∞ performance level (ξ, β) . Meanwhile, the following inequality holds for $\chi \in [1, \infty)$, $\vartheta \in [0, 1]$

$$\mathbb{E}\{\|\bar{x}(k)\|\} \leq \chi \|\bar{x}(k_0)\| \vartheta^{k-k_0} \quad (9)$$

where

$$\begin{aligned} a &\triangleq \min_{\forall s \in \mathcal{N}} \lambda_{\min}(P^{[s]}), \quad b \triangleq \max_{\forall s \in \mathcal{N}} \lambda_{\max}(P^{[s]}) \\ \vartheta &\triangleq \sqrt{\beta \varepsilon^{\frac{1}{T_a}}}, \quad \chi \triangleq \sqrt{\frac{b}{a}} \end{aligned}$$

Proof. Construct the following segmented Lyapunov function

$$\bar{V}(k) \triangleq \bar{x}^T(k) \left(\sum_{s=1}^{\mathcal{N}} \rho_s(k) P^{[s]} \right) \bar{x}(k) \quad (10)$$

where $P^{[s]}$, the predefined parameter sets, are to be designed later. For $k \in [k_\delta, k_{\delta+1})$, we construct the

following equation

$$\begin{aligned} &\mathbb{E}\left\{ \Delta \bar{V}(\bar{x}(k), \rho_s(k)) \right\} \\ &\triangleq \mathbb{E}\left\{ \bar{V}(\bar{x}(k+1), \rho_s(k+1)) - \bar{V}(\bar{x}(k), \rho_s(k)) \right\} \\ &= \mathbb{E}\left\{ \sum_{s=1}^{\mathcal{N}} \rho_s(k) \sum_{i=1}^r h_i^{[s]}(\sigma^{[s]}(k)) \sum_{j=1}^r h_j^{[s]}(\sigma^{[s]}(k)) \right. \\ &\quad \times \bar{x}(k)^T \left[(\bar{A}_{ij}^{[s]})^T P^{[s]} \bar{A}_{ij}^{[s]} + \eta (\bar{D}_{2i}^{[s]})^T P^{[s]} \bar{D}_{2i}^{[s]} \right. \\ &\quad \left. \left. - P^{[s]} \right] \bar{x}(k) + \varpi(k)^T (\bar{D}_{ij}^{[s]})^T P^{[s]} \bar{D}_{ij}^{[s]} \varpi(k) \right. \\ &\quad \left. + \bar{x}(k)^T (\bar{A}_{ij}^{[s]})^T P^{[s]} \bar{D}_{ij}^{[s]} \varpi(k) \right. \\ &\quad \left. + \varpi(k) (\bar{D}_{ij}^{[s]})^T P^{[s]} \bar{A}_{ij}^{[s]} \bar{x}(k) \right\} \end{aligned}$$

and

$$\begin{aligned} &\mathbb{E}\left\{ \Delta \bar{V}(\bar{x}(k), \rho_s(k)) - (\beta - 1) \bar{V}(\bar{x}(k), \rho_s(k)) \right\} \\ &= \mathbb{E}\left\{ \sum_{s=1}^{\mathcal{N}} \rho_s(k) \sum_{i=1}^r h_i^{[s]}(\sigma^{[s]}(k)) \sum_{j=1}^r h_j^{[s]}(\sigma^{[s]}(k)) \right. \\ &\quad \times \bar{x}(k)^T \left[(\bar{A}_{ij}^{[s]})^T P^{[s]} \bar{A}_{ij}^{[s]} + \eta (\bar{D}_{2i}^{[s]})^T P^{[s]} \bar{D}_{2i}^{[s]} \right. \\ &\quad \left. \left. - \beta P^{[s]} \right] \bar{x}(k) + \varpi(k)^T (\bar{D}_{ij}^{[s]})^T P^{[s]} \bar{D}_{ij}^{[s]} \varpi(k) \right. \\ &\quad \left. + \bar{x}(k)^T (\bar{A}_{ij}^{[s]})^T P^{[s]} \bar{D}_{ij}^{[s]} \varpi(k) \right. \\ &\quad \left. + \varpi(k) (\bar{D}_{ij}^{[s]})^T P^{[s]} \bar{A}_{ij}^{[s]} \bar{x}(k) \right\} \end{aligned}$$

By (8), we can get the following result when $\varpi(k) = 0$

$$\begin{aligned} &\mathbb{E}\left\{ \Delta \bar{V}(\bar{x}(k), \rho_s(k)) - (\beta - 1) \bar{V}(\bar{x}(k), \rho_s(k)) \right\} < 0, \\ &\quad \forall k \in [k_\delta, k_{\delta+1}), \forall s \in \mathcal{N} \end{aligned} \quad (13)$$

Let $0 < k_0 < \dots < k_\delta < \dots < k_{\mathcal{N}}$ ($\delta = 1, \dots, \mathcal{N}$) denote the segmented connection points of ρ_s on the time range $(0, k)$. Therefore, for $k \in [k_\delta, k_{\delta+1})$, we can derive that

$$\mathbb{E}\left\{ \bar{V}(\bar{x}(k), \rho_s(k)) \right\} < \beta^{k-k_\delta} \mathbb{E}\left\{ \bar{V}(\bar{x}(k_\delta), \rho_s(k_\delta)) \right\}$$

Combining (10) and (8c) acquires

$$\mathbb{E}\left\{ \bar{V}(\bar{x}(k_\delta), \rho_s(k_\delta)) \right\} < \varepsilon \mathbb{E}\left\{ \bar{V}(\bar{x}(k_{\delta-1}), \rho_s(k_{\delta-1})) \right\}$$

Therefore, one can get

$$\mathbb{E}\left\{ \bar{V}(\bar{x}(k), \rho_s(k)) \right\} \leq \beta^{k-k_0} \varepsilon^{N_a(k_0, k)} \mathbb{E}\left\{ \bar{V}(\bar{x}(k_0), \rho_s(k_0)) \right\}$$

Then, the following inequality can be obtained by considering the correlation $N_a(k_0, k) \leq \frac{k-k_0}{T_a}$, that is

$$\mathbb{E}\left\{ \bar{V}(\bar{x}(k), \rho_s(k)) \right\} \leq (\beta \varepsilon^{\frac{1}{T_a}})^{k-k_0} \mathbb{E}\left\{ \bar{V}(\bar{x}(k_0), \rho_s(k_0)) \right\}$$

Note from the definition of a and b , two positive integer a and b are available, which satisfy $a \leq b$. Thus we can get the following inequalities

$$\frac{1}{a} \mathbb{E} \left\{ \bar{\mathcal{V}}(\bar{x}(k), \rho_s(k)) \right\} \geq \mathbb{E} \left\{ \|\bar{x}(k)\|^2 \right\} \quad (14a)$$

$$\frac{1}{b} \mathbb{E} \left\{ \bar{\mathcal{V}}(\bar{x}(k_0), \rho_s(k_0)) \right\} \leq \|\bar{x}(k_0)\|^2 \quad (14b)$$

Next, the following inequality yields from (14)

$$\begin{aligned} \mathbb{E} \left\{ \|\bar{x}(k)\|^2 \right\} &\leq \frac{1}{a} \mathbb{E} \left\{ \bar{\mathcal{V}}(\bar{x}(k), \rho_s(k)) \right\} \\ &\leq \frac{b}{a} (\beta \varepsilon^{\frac{1}{T_a}})^{k-k_0} \|\bar{x}(k_0)\|^2 \end{aligned}$$

Define $\vartheta \triangleq \sqrt{\beta \varepsilon^{\frac{1}{T_a}}}$, and we can get

$$\mathbb{E} \left\{ \|\bar{x}(k)\| \right\} - \sqrt{\frac{b}{a}} \vartheta^{k-k_0} \|\bar{x}(k_0)\| \leq 0 \quad (15)$$

In addition, define $\mathcal{J}(k)$ as the below form

$$\begin{aligned} \mathcal{J}(k) \triangleq &\mathbb{E} \left\{ \Delta \bar{\mathcal{V}}(\bar{x}(k), \rho_s(k)) - (\beta - 1) \bar{\mathcal{V}}(\bar{x}(k), \rho_s(k)) \right. \\ &\left. + y_d^T(k) y_d(k) - \xi^2 \varpi^T(k) \varpi(k) \right\} \end{aligned} \quad (16)$$

The following equation can be yielded

$$\begin{aligned} \mathcal{J}(k) = &\sum_{s=1}^{\mathcal{N}} \rho_s(k) \sum_{i=1}^r h_i^{[s]}(\sigma^{[s]}(k)) \sum_{j=1}^r h_j^{[s]}(\sigma^{[s]}(k)) \\ &\times \begin{bmatrix} \bar{x}(k) \\ \varpi(k) \end{bmatrix}^T \begin{bmatrix} \Xi_{11ij}^{[s]} - \beta P^{[s]} & \Xi_{12ij}^{[s]} \\ \star & \Xi_{22ij}^{[s]} \end{bmatrix} \begin{bmatrix} \bar{x}(k) \\ \varpi(k) \end{bmatrix} \end{aligned} \quad (17)$$

where

$$\begin{aligned} \Xi_{11ij}^{[s]} &\triangleq (\bar{A}_{ij}^{[s]})^T P^{[s]} \bar{A}_{ij}^{[s]} + (\bar{C}_j^{[s]})^T \bar{C}_j^{[s]} + \eta (\bar{D}_{2i}^{[s]})^T P^{[s]} \bar{D}_{2i}^{[s]} \\ \Xi_{12ij}^{[s]} &\triangleq (\bar{A}_{ij}^{[s]})^T P^{[s]} \bar{D}_{ij}^{[s]} + (\bar{C}_j^{[s]})^T \bar{F}_0^{[s]} \\ \Xi_{22ij}^{[s]} &\triangleq (\bar{D}_{ij}^{[s]})^T P^{[s]} \bar{D}_{ij}^{[s]} + (\bar{F}_0^{[s]})^T \bar{F}_0^{[s]} - \xi^2 I \end{aligned}$$

Considering (8) and Schur's complement, we can obtain $\mathcal{J}(k) < 0$ for $k \in [k_\delta, k_{\delta+1})$. Define $\Lambda(k) \triangleq y_d^T(k) y_d(k) - \xi^2 \varpi^T(k) \varpi(k)$, and the following inequality can be derived

$$\mathbb{E} \left\{ \Delta \bar{\mathcal{V}}(\bar{x}(k), \rho_s(k)) \right\} < \mathbb{E} \left\{ (\beta - 1) \bar{\mathcal{V}}(\bar{x}(k), \rho_s(k)) - \Lambda(k) \right\}$$

For $k \in [k_\delta, k_{\delta+1})$, we obtain

$$\begin{aligned} \mathbb{E} \left\{ \bar{\mathcal{V}}(\bar{x}(k), \rho_s(k)) \right\} &< \beta^{k-k_\delta} \mathbb{E} \left\{ \bar{\mathcal{V}}(\bar{x}(k_\delta), \rho_s(k_\delta)) \right\} \\ &\quad - \mathbb{E} \left\{ \sum_{s=k_\delta}^{k-1} \beta^{k-1-s} \Lambda(k) \right\} \\ &\quad \dots \\ \mathbb{E} \left\{ \bar{\mathcal{V}}(\bar{x}(k_1), \rho_s(k_1)) \right\} &< \beta^{k_1-k_0} \varepsilon \mathbb{E} \left\{ \bar{\mathcal{V}}(\bar{x}(k_0), \rho_s(k_0)) \right\} \\ &\quad - \varepsilon \mathbb{E} \left\{ \sum_{s=k_0}^{k_1-1} \beta^{k_1-1-s} \Lambda(k) \right\} \end{aligned}$$

Since $N_a(k_0, k) \leq \frac{k-k_0}{T_a}$, we get

$$\begin{aligned} \mathbb{E} \left\{ \bar{\mathcal{V}}(\bar{x}(k), \rho_s(k)) \right\} &< \mathbb{E} \left\{ \beta^{k-k_0} \varepsilon^{N_a(k_0, k)} \bar{\mathcal{V}}(\bar{x}(k_0), \rho_s(k_0)) \right. \\ &\quad \left. - \sum_{s=k_0}^{k-1} \beta^{k-1-s} \varepsilon^{N_a(k_0, k)} \Lambda(k) \right\} \end{aligned}$$

Then, the above inequality implies

$$\mathbb{E} \left\{ \sum_{s=k_0}^{k-1} \beta^{k-1-s} \varepsilon^{-N_a(0, s)} \left(y_d^T(k) y_d(k) - \xi^2 \varpi^T(k) \varpi(k) \right) \right\} < 0$$

Note that $N_a(0, s) \leq \frac{s}{T_a}$ and $T_a \geq -\frac{\ln \varepsilon}{\ln \beta}$, so the above inequality can be converted to the following inequality

$$\begin{aligned} &\mathbb{E} \left\{ \sum_{s=k_0}^{k-1} \beta^{k-1-s} \varepsilon^{\frac{\ln \beta}{\ln \varepsilon} s} y_d^T(k) y_d(k) \right\} \\ &< \xi^2 \mathbb{E} \left\{ \sum_{s=k_0}^{k-1} \beta^{k-1-s} \varpi^T(k) \varpi(k) \right\} \end{aligned}$$

Finally, we can obtain a significant result, that is

$$\mathbb{E} \left\{ \sum_{s=k_0}^{\infty} \beta^s y_d^T(s) y_d(s) \right\} < \xi^2 \mathbb{E} \left\{ \sum_{s=k_0}^{\infty} \varpi^T(s) \varpi(s) \right\} \quad (18)$$

Therefore, the dynamic residual system (4) is proved to have mean-square exponentially stability with a balanced \mathcal{H}_∞ performance level (ξ, β) . This completes the proof. \square

Remark 2. The number of parameter $P^{[s]}$ ($s \in 1, 2, \dots, \mathcal{N}$) of the Lyapunov function $\bar{\mathcal{V}}(k)$ designed in this paper is consistent with the number of switching systems, so that $P^{[s]}$ is a set of parameters rather than a fixed value. In practical application, if there are many switching subsystems, the determination of parameter $P^{[s]}$ will be more difficult. Therefore, how to strike a balance between reducing conservatism and simplifying $P^{[s]}$ is worth studying in the future.

IV. Dynamic Fault Detector and Controller Design

In this section, the FRFDC are designed and discussed, and the differences between the design processes of full- and reduced-order system are analyzed. Subsequently, some discussions and explanations of these two methods are listed.

A. Full-order Fault Detectors and Controllers Design

In this subsection, we identify a general design criterion to address the full-order fault detector and controller design problem of the system defined in (4).

Theorem 2. Given scalars $\xi > 0$, $0 < \beta < 1$ and $\varepsilon \geq 1$, supposing there exist $\mathcal{S}^{[s]}$, $\mathcal{W}^{[s]}$, $A_{fj}^{[s]}$, $B_{fj}^{[s]}$, $C_{fj}^{[s]}$ and $K_{fj}^{[s]}$ such that the below formulas hold for $l, s \in \mathcal{N}$

$$\tilde{\Omega}_{ii} < 0, \quad i = 1, 2, \dots, r \quad (19a)$$

$$\frac{1}{r-1}\tilde{\Omega}_{ii}^{[s]} + \frac{1}{2}(\tilde{\Omega}_{ij}^{[s]} + \tilde{\Omega}_{ji}^{[s]}) < 0, \quad 1 \leq i < j \leq r \quad (19b)$$

$$P^{[s]} - \varepsilon P^{[l]} \leq 0, \quad \forall s, l \in \mathcal{N} \quad (19c)$$

$$P^{[s]} Q^{[s]} - I = 0 \quad (19d)$$

where

$$\tilde{\Omega}_{ij} \triangleq \begin{bmatrix} \tilde{\Upsilon}_{110} & \tilde{\Upsilon}_{2ij} \\ \star & \tilde{\Upsilon}_{330} \end{bmatrix}, \quad \tilde{\Upsilon}_{110} \triangleq \begin{bmatrix} -\beta \mathcal{P}_0^{[s]} & 0 \\ 0 & -\xi^2 I \end{bmatrix}$$

$$\tilde{\Upsilon}_{2ij} \triangleq \begin{bmatrix} (\tilde{A}_{ij}^{[s]})^T & (\tilde{C}_j^{[s]})^T & (\tilde{D}_{2i}^{[s]})^T \\ (\tilde{D}_{ij}^{[s]})^T & (F_0^{[s]})^T & 0 \end{bmatrix}$$

$$\tilde{\Upsilon}_{330} \triangleq \begin{bmatrix} -\mathcal{Q}_0^{[s]} & 0 & 0 \\ 0 & -I & 0 \\ 0 & 0 & -\frac{1}{\eta} \mathcal{Q}_0^{[s]} \end{bmatrix}$$

then, the full-order dynamic residual system (4) is MSES with a balanced \mathcal{H}_∞ performance level (ξ, β) . Furthermore, the full-order parameters can be constructed by:

$$\begin{bmatrix} A_{fj}^{[s]} & B_{fj}^{[s]} \\ C_{fj}^{[s]} & 0 \\ K_{fj}^{[s]} & 0 \end{bmatrix} \triangleq \begin{bmatrix} (\mathcal{R}^{[s]})^{-1} & 0 & -(\mathcal{R}^{[s]})^{-1}(\mathcal{S}^{[s]})^T B_i^{[s]} \\ 0 & I & 0 \\ 0 & 0 & I \end{bmatrix}$$

$$\times \begin{bmatrix} \mathcal{A}_{fj}^{[s]} - (\mathcal{S}^{[s]})^T A_i^{[s]} \mathcal{W}^{[s]} & \mathcal{B}_{fj}^{[s]} \\ C_{fj}^{[s]} & 0 \\ \mathcal{K}_{fj}^{[s]} & 0 \end{bmatrix}$$

$$\times \begin{bmatrix} (\mathcal{X}^{[s]})^{-T} & 0 \\ -C_i^{[s]} \mathcal{W}^{[s]} (\mathcal{X}^{[s]})^{-T} & I \end{bmatrix}$$

Proof. Let

$$P^{[s]} \triangleq \begin{bmatrix} \mathcal{S}^{[s]} & \mathcal{R}^{[s]} \\ (\mathcal{R}^{[s]})^T & \mathcal{T}^{[s]} \end{bmatrix}, \quad Q^{[s]} \triangleq \begin{bmatrix} \mathcal{W}^{[s]} & \mathcal{X}^{[s]} \\ (\mathcal{X}^{[s]})^T & \mathcal{V}^{[s]} \end{bmatrix}$$

and

$$\mathcal{F}_P^{[s]} \triangleq \begin{bmatrix} \mathcal{S}^{[s]} & I \\ (\mathcal{R}^{[s]})^T & 0 \end{bmatrix}, \quad \mathcal{F}_Q^{[s]} \triangleq \begin{bmatrix} I & \mathcal{W}^{[s]} \\ 0 & (\mathcal{X}^{[s]})^T \end{bmatrix}$$

One has $\mathcal{F}_Q^{[s]} = (P^{[s]})^{-1} \mathcal{F}_P^{[s]}$, $\mathcal{F}_P^{[s]} = (Q^{[s]})^{-1} \mathcal{F}_Q^{[s]}$. Introducing

$$\mathbb{W} \triangleq \text{diag}\{\mathcal{F}_Q^{[s]}, I, \mathcal{F}_P^{[s]}, I, \mathcal{F}_P^{[s]}\}$$

the following equations can be obtained by performing congruence transformations to (8a)-(8b) by \mathbb{W}

$$(\tilde{A}_{ij}^{[s]})^T \triangleq (\mathcal{F}_Q^{[s]})^T (\tilde{A}_{ij}^{[s]})^T \mathcal{F}_P^{[s]}, \quad (\tilde{D}_{ij}^{[s]})^T \triangleq (\tilde{D}_{ij}^{[s]})^T \mathcal{F}_P^{[s]}$$

$$(\tilde{D}_{2i}^{[s]})^T \triangleq (\mathcal{F}_Q^{[s]})^T (\tilde{D}_{2i}^{[s]})^T \mathcal{F}_P^{[s]}, \quad (\tilde{C}_j^{[s]})^T \triangleq (\mathcal{F}_Q^{[s]})^T (\tilde{C}_j^{[s]})^T$$

$$\mathcal{P}_0^{[s]} \triangleq (\mathcal{F}_Q^{[s]})^T (P^{[s]})^T \mathcal{F}_Q^{[s]}, \quad \mathcal{Q}_0^{[s]} \triangleq (\mathcal{F}_P^{[s]})^T (Q^{[s]})^T \mathcal{F}_P^{[s]}$$

Thus we obtain the following expanded forms

$$(\tilde{A}_{ij}^{[s]})^T = \begin{bmatrix} \mathcal{Y}_{11} & (A_i^{[s]})^T \\ (\mathcal{A}_{fj}^{[s]})^T & \mathcal{Y}_{22} \end{bmatrix}, \quad \mathcal{P}_0^{[s]} = \begin{bmatrix} \mathcal{S}^{[s]} & I \\ I & \mathcal{W}^{[s]} \end{bmatrix}$$

$$(\tilde{D}_{2i}^{[s]})^T = \begin{bmatrix} (D_{2i}^{[s]})^T \mathcal{S}^{[s]} & (D_{2i}^{[s]})^T \\ (\mathcal{D}_{2i}^{[s]})^T \mathcal{S}^{[s]} & (\mathcal{D}_{2i}^{[s]})^T \end{bmatrix}, \quad \mathcal{Q}_0^{[s]} = \mathcal{P}_0^{[s]}$$

$$(\tilde{D}_{ij}^{[s]})^T = \begin{bmatrix} \mathcal{Y}_{33} & (D_{1i}^{[s]})^T \\ \mathcal{Y}_{44} & (E_i^{[s]})^T \end{bmatrix}, \quad (\tilde{C}_j^{[s]})^T = \begin{bmatrix} 0 \\ (C_{fj}^{[s]})^T \end{bmatrix}$$

$$(\mathcal{D}_{2i}^{[s]})^T = (\mathcal{W}^{[s]})^T (D_{2i}^{[s]})^T$$

$$\mathcal{Y}_{11} = (A_i^{[s]})^T \mathcal{S}^{[s]} + (C_i^{[s]})^T (\mathcal{B}_{fj}^{[s]})^T,$$

$$\mathcal{Y}_{22} = (\mathcal{W}^{[s]})^T (A_i^{[s]})^T + (\mathcal{K}_{fj}^{[s]})^T (B_i^{[s]})^T$$

$$\mathcal{Y}_{33} = (D_{1i}^{[s]})^T \mathcal{S}^{[s]} + (L_i^{[s]})^T (\mathcal{B}_{fj}^{[s]})^T$$

$$\mathcal{Y}_{44} = (E_i^{[s]})^T \mathcal{S}^{[s]} + (F_i^{[s]})^T (\mathcal{B}_{fj}^{[s]})^T$$

Till now, the proof of Theorem 2 is completed. \square

Remark 3. Because $\mathcal{S}^{[s]}$ and $\mathcal{W}^{[s]}$ are known, two nonsingular matrices $\mathcal{R}^{[s]}$ and $\mathcal{X}^{[s]}$ can be obtained by solving the following equation

$$\mathcal{R}^{[s]} (\mathcal{X}^{[s]})^T = I - \mathcal{S}^{[s]} \mathcal{W}^{[s]}$$

$\mathcal{S}^{[s]}$, $\mathcal{R}^{[s]}$, $\mathcal{T}^{[s]}$, $\mathcal{W}^{[s]}$, $\mathcal{X}^{[s]}$, and $\mathcal{V}^{[s]}$ have the same dimensions ($n \times n$) as the system state matrix. Considering $P^{[s]} Q^{[s]} = I$, the following equation can be derived:

$$(\mathcal{R}^{[s]})^T \mathcal{W}^{[s]} + \mathcal{T}^{[s]} (\mathcal{X}^{[s]})^T = 0$$

Remark 4. Apparently, Eq. (17) can be converted into linear matrix inequalities after using Schur complement lemma, which can be solved directly through the linear matrix inequality toolbox in MATLAB. In order to reflect the design differences between full- and reduced-order residual system, Theorem 1 is linearized and the design of full-order fault detector and controller in Theorem 2 is obtained. Then, by introducing matrix \mathcal{E} , it plays an critical role in the design of reduced-order fault detector and controller. Finally, the corresponding allowable performance parameters (ξ, β) , and the parameters A_{fj} , B_{fj} , C_{fj} and K_{fj} are designed from the derived results, which can be readily solved by using standard numerical software.

B. Reduced-order Fault Detectors and Controllers Design

On the basis of full-order fault detector and controller, we establish a method to design the reduced-order fault detector and controller.

Theorem 3. Given scalars $\xi > 0$, $0 < \beta < 1$ and $\varepsilon \geq 1$, supposing there exist $\mathcal{S}^{[s]}$, $\mathcal{W}^{[s]}$, $\tilde{A}_{fj}^{[s]}$, $\tilde{B}_{fj}^{[s]}$, $\tilde{C}_{fj}^{[s]}$ and $\tilde{K}_{fj}^{[s]}$ such that the following formulas hold for $l, s \in \mathcal{N}$

$$\tilde{\Omega}_{ii} < 0, \quad i = 1, 2, \dots, r \quad (20a)$$

$$\frac{1}{r-1}\tilde{\Omega}_{ii}^{[s]} + \frac{1}{2}(\tilde{\Omega}_{ij}^{[s]} + \tilde{\Omega}_{ji}^{[s]}) < 0, \quad 1 \leq i < j \leq r \quad (20b)$$

$$\mathcal{P}^{[s]} - \varepsilon \mathcal{P}^{[l]} \leq 0, \quad \forall s, l \in \mathcal{N} \quad (20c)$$

$$\mathcal{P}^{[s]} \mathcal{Q}^{[s]} - I = 0 \quad (20d)$$

where

$$\begin{aligned}\check{\Omega}_{ij} &\triangleq \begin{bmatrix} \check{\Upsilon}_{110} & \check{\Upsilon}_{2ij} \\ \star & \check{\Upsilon}_{330} \end{bmatrix}, \quad \check{\Upsilon}_{110} \triangleq \begin{bmatrix} -\beta\bar{\mathcal{P}}_0^{[s]} & 0 \\ 0 & -\xi^2 I \end{bmatrix} \\ \check{\Upsilon}_{2ij} &\triangleq \begin{bmatrix} (\check{A}_{ij}^{[s]})^T & (\check{C}_j^{[s]})^T & (\check{D}_{2i}^{[s]})^T \\ (\check{D}_{ij}^{[s]})^T & (\check{F}_0^{[s]})^T & 0 \end{bmatrix} \\ \check{\Upsilon}_{330} &\triangleq \begin{bmatrix} -\check{\mathcal{Q}}_0^{[s]} & 0 & 0 \\ 0 & -I & 0 \\ 0 & 0 & -\frac{1}{\eta}\check{\mathcal{Q}}_0^{[s]} \end{bmatrix}\end{aligned}$$

then, the reduced-order dynamic residual system (4) is MSES with a balanced \mathcal{H}_∞ performance level (ξ, β) . Furthermore, the reduced-order parameters are given by:

$$\begin{aligned}\check{A}_{fj}^{[s]} &\triangleq (\mathcal{E}\mathcal{R}^{[s]})^{-1} \left(\check{A}_{fj}^{[s]} - (\mathcal{S}^{[s]})^T A_i^{[s]} \mathcal{W}^{[s]} - \check{B}_{fj}^{[s]} C_i^{[s]} \mathcal{W}^{[s]} \right. \\ &\quad \left. - (\mathcal{S}^{[s]})^T B_i^{[s]} \check{\mathcal{K}}_{fj}^{[s]} \right) (\mathcal{E}\mathcal{X}^{[s]})^{-T} \\ \check{B}_{fj}^{[s]} &\triangleq (\mathcal{R}^{[s]})^{-1} \check{B}_{fj}^{[s]}, \quad \check{C}_{fj}^{[s]} \triangleq \check{C}_{fj}^{[s]} (\mathcal{X}^{[s]})^{-T} \\ \check{K}_{fj}^{[s]} &\triangleq \check{\mathcal{K}}_{fj}^{[s]} (\mathcal{X}^{[s]})^{-T}\end{aligned} \quad \min \varsigma$$

Proof. Redefine $\bar{\mathcal{F}}_P^{[s]}$ and $\bar{\mathcal{F}}_Q^{[s]}$ as:

$$\bar{\mathcal{F}}_P^{[s]} \triangleq \begin{bmatrix} \mathcal{S}^{[s]} & I \\ (\mathcal{E}\mathcal{R}^{[s]})^T & 0 \end{bmatrix}, \quad \bar{\mathcal{F}}_Q^{[s]} \triangleq \begin{bmatrix} I & \mathcal{W}^{[s]} \\ 0 & (\mathcal{E}\mathcal{X}^{[s]})^T \end{bmatrix} \quad (21)$$

Performing congruence transformations to (8a)-(8b) by $\bar{\mathbb{W}} \triangleq \text{diag}\{\bar{\mathcal{F}}_Q^{[s]}, I, \bar{\mathcal{F}}_P^{[s]}, I, \bar{\mathcal{F}}_P^{[s]}\}$, one obtains

$$\begin{aligned}(\check{A}_{ij}^{[s]})^T &= \begin{bmatrix} \bar{\mathcal{Y}}_{11} & (A_i^{[s]})^T \\ (A_{fj}^{[s]})^T & \bar{\mathcal{Y}}_{22} \end{bmatrix}, \quad \bar{\mathcal{P}}_0^{[s]} = \mathcal{P}_0^{[s]} \\ (\check{D}_{2i}^{[s]})^T &= \begin{bmatrix} (D_{2i}^{[s]})^T \mathcal{S}^{[s]} & (D_{2i}^{[s]})^T \\ (D_{2i}^{[s]})^T \mathcal{S}^{[s]} & (D_{2i}^{[s]})^T \end{bmatrix}, \quad \bar{\mathcal{Q}}_0^{[s]} = \mathcal{Q}_0^{[s]} \\ (\check{D}_{ij}^{[s]})^T &= \begin{bmatrix} \bar{\mathcal{Y}}_{33} & (D_{1i}^{[s]})^T \\ \bar{\mathcal{Y}}_{44} & (E_i^{[s]})^T \end{bmatrix}, \quad (\check{C}_j^{[s]})^T = \begin{bmatrix} 0 \\ \mathcal{E}(C_{fj}^{[s]})^T \end{bmatrix} \\ (\mathcal{D}_{2i}^{[s]})^T &= (\mathcal{W}^{[s]})^T (D_{2i}^{[s]})^T \\ \bar{\mathcal{Y}}_{11} &= (A_i^{[s]})^T \mathcal{S}^{[s]} + (C_i^{[s]})^T (\mathcal{B}_{fj}^{[s]})^T \mathcal{E}^T \\ \bar{\mathcal{Y}}_{22} &= (\mathcal{W}^{[s]})^T (A_i^{[s]})^T + \mathcal{E}(\mathcal{K}_{fj}^{[s]})^T (B_i^{[s]})^T \\ \bar{\mathcal{Y}}_{33} &= (D_{1i}^{[s]})^T \mathcal{S}^{[s]} + (L_i^{[s]})^T (\mathcal{B}_{fj}^{[s]})^T \mathcal{E}^T \\ \bar{\mathcal{Y}}_{44} &= (E_i^{[s]})^T \mathcal{S}^{[s]} + (F_i^{[s]})^T (\mathcal{B}_{fj}^{[s]})^T \mathcal{E}^T\end{aligned}$$

The results in Theorem 3 can be obtained easily based on the above equations. Therefore, the proof is completed. \square

Remark 5. Considering $\mathcal{E} = [I_{k \times k} \quad 0_{k \times (n-k)}]^T$, the dimensions of the parameters can be modified to $\mathcal{S}_{n \times n}^{[s]}$, $(\mathcal{E}\mathcal{R}^{[s]})_{n \times k}$, $\mathcal{T}_{k \times k}^{[s]}$, $\mathcal{W}_{n \times n}^{[s]}$, $(\mathcal{E}\mathcal{X}^{[s]})_{n \times k}$, and $\mathcal{V}_{k \times k}^{[s]}$, in which k is the desired dimension of the state matrix of the control system. To ensure the validity of the solution, we assume that $\mathcal{R}_{k \times k}^{[s]}$ and $\mathcal{X}_{k \times k}^{[s]}$ are nonsingular. Otherwise, we consider $\mathcal{R}_{k \times k}^{[s]} + \Delta\mathcal{R}_{k \times k}^{[s]}$ and $\mathcal{X}_{k \times k}^{[s]} + \Delta\mathcal{X}_{k \times k}^{[s]}$, where

$\Delta\mathcal{R}_{k \times k}^{[s]}$ and $\Delta\mathcal{X}_{k \times k}^{[s]}$ are adequate small matrices. In such a case, $\bar{\mathcal{F}}_P^{[s]}$ and $\bar{\mathcal{F}}_Q^{[s]}$ remain valid. Additionally, Theorem 3 transforms to Theorem 2 when $n = k$.

Remark 6. Note that another method commonly used in reduced-order controller design is to use projection lemma [38], [39]. The design results obtained using this technique are usually represented in the form of linear matrix inequalities plus an additional rank constraint. Since the rank constraint is non-convex, it is difficult to meet this condition using numerical software. In this paper, we solve the FRFDC design problem by using a linearization technology, which can be realized by available software. Therefore, the target FRFDC is designed by solving:

$$\text{subject to (19) or (20) with } \varsigma = \xi^2$$

Remark 7. Compared with [12]–[14], the number of subsystems of this paper is $r\mathcal{N}$. Besides, a set of switching fuzzy output feedback controllers are designed while considering the fault detection in this paper. It can be noted that this paper does not directly use the original system states for state feedback control, which is more practical for the system whose state variables cannot be directly monitored.

Remark 8. The time complexity level of the proposed method is $O(\mathcal{N}rm^3)$. Note that the complexity of the dynamic residual system is mainly determined by the dimensions of the system state matrix m , the number of fuzzy rules r and switching subsystems \mathcal{N} . It can be seen that the increase of m means that the operation times of the dynamic residual system will increase, and the increase of r or \mathcal{N} means that the iteration times of the dynamic residual system increases. Undoubtedly, they are closely related to the computational complexity of the algorithm in this paper.

V. Illustrative Examples

In this section, two examples are considered, namely a numerical example and a practical example. The second example aims to verify the applicability of fault detector and controller design technique in a switching Chua's circuit system.

Example 1. Consider the number of switching subsystems as 2, and the parameters are given as:

Subsystem 1.

$$\begin{aligned}
 A_1^{[1]} &= \begin{bmatrix} -0.4 & 0.1 & 0.4 \\ 0.3 & 0.8 & 0.1 \\ 0.1 & 0.5 & 0.6 \end{bmatrix}, & D_{11}^{[1]} &= \begin{bmatrix} 0.1 \\ 0.2 \\ -0.1 \end{bmatrix} \\
 A_2^{[1]} &= \begin{bmatrix} -0.6 & 0.1 & 0.3 \\ 0.3 & 0.6 & 0.5 \\ 0.2 & 0.5 & 0.8 \end{bmatrix}, & D_{12}^{[1]} &= \begin{bmatrix} 0.1 \\ 0.1 \\ 0.3 \end{bmatrix} \\
 D_{21}^{[1]} &= \begin{bmatrix} 0.01 & 0.01 & 0.02 \\ 0.01 & 0.03 & 0 \\ 0 & 0.02 & 0.01 \end{bmatrix}, & B_1^{[1]} &= \begin{bmatrix} 0.1 \\ 0.2 \\ 0.5 \end{bmatrix} \\
 D_{22}^{[1]} &= \begin{bmatrix} 0.01 & 0.01 & 0.02 \\ 0.01 & 0.03 & 0 \\ 0 & 0.02 & 0.01 \end{bmatrix}, & B_2^{[1]} &= \begin{bmatrix} 0.3 \\ 0.1 \\ 0.4 \end{bmatrix} \\
 E_1^{[1]} &= [0.1 \ 0.1 \ 0.1]^T, & E_2^{[1]} &= [0.1 \ 0.1 \ 0.1]^T \\
 C_1^{[1]} &= [0.6 \ 0.2 \ 1.8]^T, & C_2^{[1]} &= [0.8 \ 0.2 \ 1.2]^T \\
 L_1^{[1]} &= 0.3, \quad L_2^{[1]} = 0.1, & F_1^{[1]} &= 0.1, \quad F_2^{[1]} = 0.2
 \end{aligned}$$

Subsystem 2.

$$\begin{aligned}
 A_1^{[2]} &= \begin{bmatrix} -0.5 & 0.1 & 0.4 \\ 0.3 & 0.6 & 0.1 \\ 0.3 & 0.2 & 0.6 \end{bmatrix}, & D_{11}^{[2]} &= \begin{bmatrix} 0.2 \\ 0.1 \\ 0.1 \end{bmatrix} \\
 A_2^{[2]} &= \begin{bmatrix} -0.4 & 0.1 & 0.2 \\ 0.3 & 0.8 & 0.4 \\ 0.3 & 0.5 & 0.8 \end{bmatrix}, & D_{12}^{[2]} &= \begin{bmatrix} 0.1 \\ 0.2 \\ 0.1 \end{bmatrix} \\
 D_{21}^{[2]} &= \begin{bmatrix} 0.03 & 0.01 & 0.02 \\ 0.01 & 0.03 & 0.02 \\ 0.01 & 0.02 & 0.01 \end{bmatrix}, & B_1^{[2]} &= \begin{bmatrix} 0.1 \\ 0.3 \\ 0.4 \end{bmatrix} \\
 D_{22}^{[2]} &= \begin{bmatrix} 0.01 & 0.01 & 0.02 \\ 0.01 & 0.03 & 0.01 \\ 0 & 0.02 & 0.01 \end{bmatrix}, & B_2^{[2]} &= \begin{bmatrix} 0.2 \\ 0.1 \\ 0.5 \end{bmatrix} \\
 E_1^{[2]} &= [0.1 \ 0.1 \ 0.1]^T, & E_2^{[2]} &= [0.1 \ 0.1 \ 0.1]^T \\
 C_1^{[2]} &= [0.6 \ 0.2 \ 1.4]^T, & C_2^{[2]} &= [0.7 \ 0.2 \ 1.6]^T \\
 L_1^{[2]} &= 0.2, \quad L_2^{[2]} = 0.1, & F_1^{[2]} &= 0.1, \quad F_2^{[2]} = 0.3
 \end{aligned}$$

In addition, select the following equations as the fuzzy membership functions:

$$\begin{aligned}
 h_1^{[s]}(x_1^{[s]}(k)) &\triangleq \frac{(1 + \sin^2(x_1^{[s]}(k)))}{2} \\
 h_2^{[s]}(x_1^{[s]}(k)) &\triangleq \frac{(1 - \sin^2(x_1^{[s]}(k)))}{2}
 \end{aligned}$$

Besides, $d(k)$ and $f(k)$ are selected as:

$$\begin{aligned}
 d(k) &= 0.1 \exp(-0.25k) \sin(0.4k), & k > 0 \\
 &= 0.05 + 0.001 \sin(k), & 40 \leq k \leq 60 \\
 f(k) &= \begin{cases} 0.06 \sqrt{56.25 - 0.09(k-80)^2}, & 70 \leq k \leq 90 \\ 0, & \text{otherwise} \end{cases}
 \end{aligned}$$

Case 1: In this case, the full-order fault detector and controller is solved. The minimum feasible scalar ξ is obtained as $\xi_{min} = 1.0053$. The simulation results are shown in Figs. 2-6. Figs. 2 and 3 display the states change of the full-order dynamic residual system. The

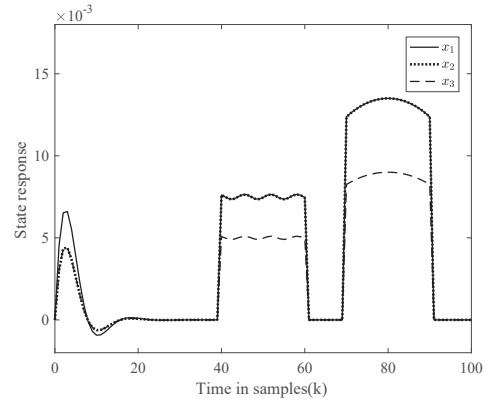


Fig. 2. The states of the original system in Case 1

control input $u(k)$, residual signal $y_d(k)$, and evaluation function $F(y_d)$ are shown in Figs. 4-6, respectively. From the simulation results, it can be seen that the states of the dynamic residual system eventually tend to be stable. When a fault signal occurs, the fault detector can respond quickly by setting an appropriate threshold F_{th} . The setting of a threshold can refer to our previous work [10].

Case 2: In this case, the reduced-order fault detector and controller is derived. We obtain the minimum feasible scalar ξ as $\xi_{min} = 1.0097$. The simulation results are shown in Figs. 7-10. Fig. 7 presents the states of the fault detection and control system, in which the number of states is reduced to 2, which is the significance of using the order reduction method. The control input $u(k)$ is depicted in Fig. 8. The control input is significantly smaller than that in the full-order system, which means that the reduced-order dynamic residual system can be better applied to the actual system with control input constraints. Figs. 9 and 10 show the residual signal $y_d(k)$ and residual evaluation function $F(y_d)$, respectively. When there are no faults, the value of the residual evaluation function of the reduced-order residual system is smaller than that of the full-order residual system. This find means that the reduced-order residual system is more sensitive to small amplitude fault signals, that is, the selection of thresholds F_{th} is more flexible.

Example 2. A switching Chua's circuit system [40] is used to verify the effectiveness of the proposed method. The original system is characterized by

$$\begin{cases} \dot{V}_1 = \frac{-1}{C_{1\kappa}R} V_1 + \frac{1}{C_{1\kappa}R} V_2 - \frac{1}{C_{1\kappa}} G_\kappa(V_1) - \frac{1}{C_{1\kappa}} u \\ \dot{V}_2 = \frac{1}{C_2R} V_1 - \frac{1}{C_2R} V_2 - \frac{1}{C_2} i_L \\ \dot{i}_L = \frac{1}{L} V_2 - \frac{1}{L} V_d \end{cases} \quad (22)$$

where $C_{1\kappa}$ and $G_\kappa(V_1)$ ($\kappa = 1, 2$) are the κ th capacitor and the i th current flowing through the nonlinear resistor $R_{nl\kappa}$, respectively. V_1 and V_2 are the voltage across the capacitors $C_{1\kappa}$ and C_2 , respectively. i_L is the current flowing through the inductor L . u is the current from generator as active control action of circuit, and V_d denotes

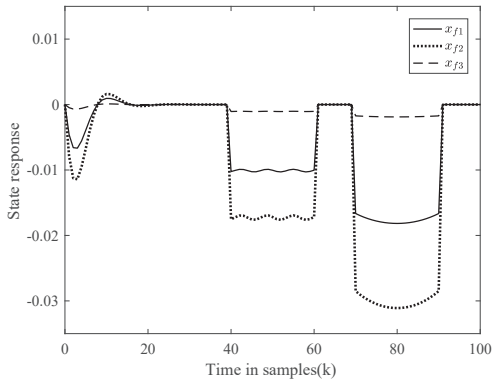


Fig. 3. The states of the control system in Case 1

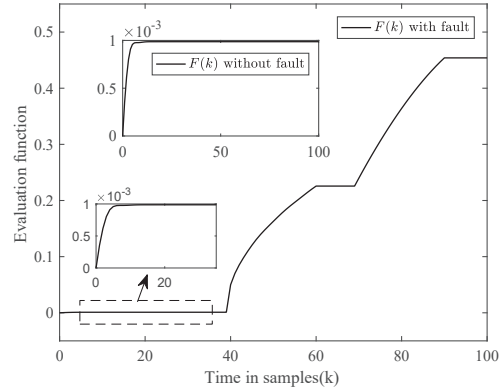


Fig. 6. Residual evaluation function $F(y_d)$ in Case 1

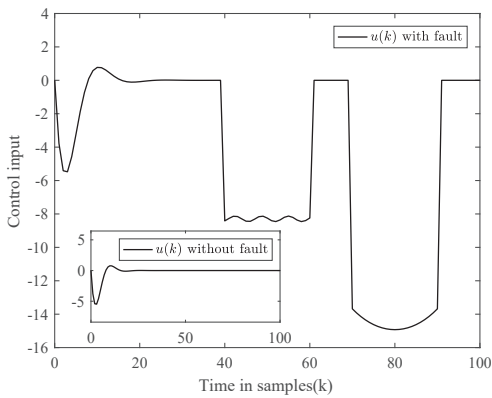


Fig. 4. Control input $u(k)$ in Case 1

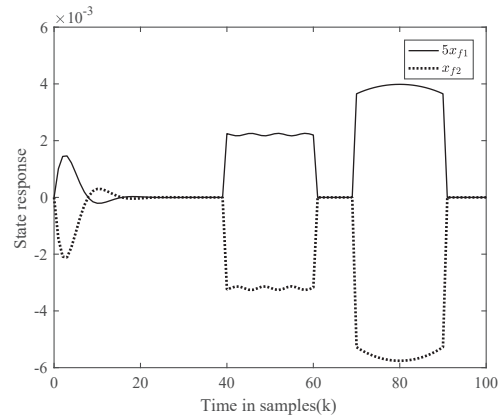


Fig. 7. The states of the control system in Case 2

voltage loss $R_0 i_L$ (R_0 is a constant resistance). In this paper, we assume that $G_t(V_1)$ has the following form:

$$G_\kappa(V_1) = \Lambda_b V_1 + \Lambda_a V_1 \omega(t) + \frac{1}{2}(\Lambda_a - \Lambda_b)(|V_1 + \bar{V}| - |V_1 - \bar{V}|)$$

where $\Lambda_a, \Lambda_b < 0$. To obtain a fuzzy model, we assume

$V_1 \in [-v_0, v_0]$, and then $G_\kappa(V_1)$ can be rewritten as

$$G_\kappa(V_1) = \begin{cases} \Lambda_a V_1 \omega(t) + \Lambda_b V_1 - (\Lambda_a - \Lambda_b) \bar{V}, & V_1 \leq -\bar{V} \\ \Lambda_a V_1 \omega(t) + \Lambda_a V_1, & -\bar{V} < V_1 < \bar{V} \\ \Lambda_a V_1 \omega(t) + \Lambda_b V_1 + (\Lambda_a - \Lambda_b) \bar{V}, & V_1 \geq \bar{V} \end{cases}$$

Therefore, the following sector to bound $G_\kappa(V_1)$ can be

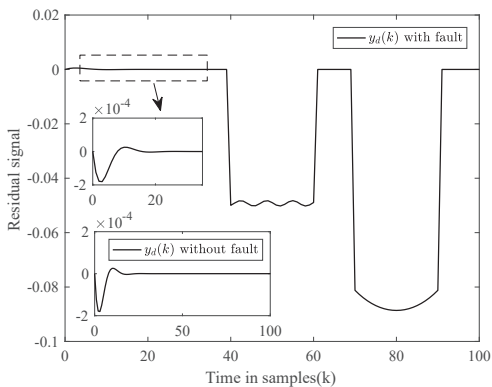


Fig. 5. Residual signal $y_d(k)$ in Case 1

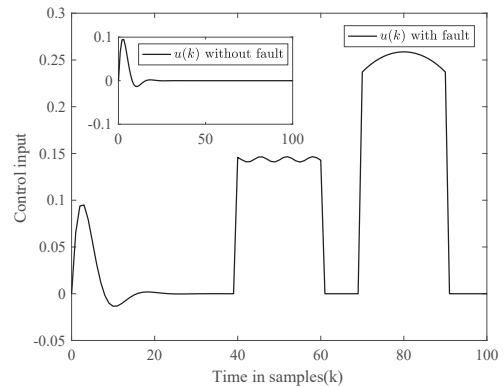


Fig. 8. Control input $u(k)$ in Case 2

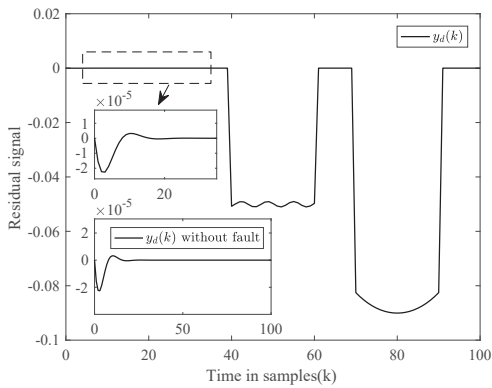


Fig. 9. Residual signal $y_d(k)$ in Case 2

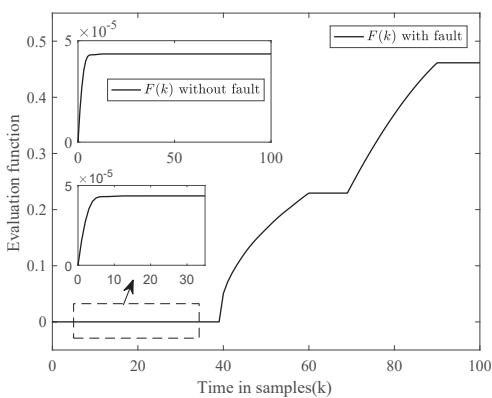


Fig. 10. Residual evaluation function $F(y_d)$ in Case 2

obtained:

$$\begin{aligned} G_1(V_1) &= \Lambda_a V_1 \omega(t) + \Lambda_a V_1 \\ G_2(V_1) &= \Lambda_a V_1 \omega(t) + \Lambda_v V_1 \end{aligned}$$

where $\Lambda_v = \Lambda_b + \frac{(\Lambda_a - \Lambda_b)\bar{V}}{v_0}$. With $\Lambda_a \neq \Lambda_b$, we can obtain the membership functions as following

$$\mathcal{W}_1(V_1) = \begin{cases} \frac{-\bar{V} - (\bar{V}/v_0)V_1}{[1 - (\bar{V}/v_0)]V_1}, & V_1 \leq -\bar{V} \\ 1, & |V_1| < \bar{V} \\ \frac{\bar{V} - (\bar{V}/v_0)V_1}{[1 - (\bar{V}/v_0)]V_1}, & V_1 \geq \bar{V} \end{cases}$$

$$\mathcal{W}_2(V_1) = 1 - \mathcal{W}_1(V_1).$$

Denote $x(t) = [V_1(t), V_2(t), i_L(t)]$, and a discrete-time switching fuzzy model can be approximately formulated using the Euler method. Specifically, $A_k = I + A_t T$, where A_k and A_t denote the state matrix of the expected discrete-time model and original continues-time model, respectively. In the same way, $B_k = B_t T$. Then, the discrete-time switching fuzzy model parameters can be

obtained as:

$$\begin{aligned} A_1^{[s]} &= \begin{bmatrix} M_s - \frac{\Lambda_a T}{C_{1s}} & \frac{T}{C_{1s} R} & 0 \\ \frac{T}{C_2 R} & \frac{-T}{C_2 R} & \frac{T}{C_2} \\ 0 & \frac{T}{L} & \frac{-TR_0}{L} \end{bmatrix}, \quad M_s = 1 - \frac{T}{C_{1s} R} \\ A_2^{[s]} &= \begin{bmatrix} M_s - \frac{\Lambda_v T}{C_{1s}} & \frac{T}{C_{1s} R} & 0 \\ \frac{T}{C_2 R} & \frac{-T}{C_2 R} & \frac{T}{C_2} \\ 0 & \frac{T}{L} & \frac{-TR_0}{L} \end{bmatrix}, \quad C_i^{[s]} = \begin{bmatrix} 1 \\ 0 \\ 0 \end{bmatrix}^T \\ D_{2i}^{[s]} &= \begin{bmatrix} 1 + \Lambda_a T & 0 & 0 \\ 0 & 0 & 0 \\ 0 & 0 & 0 \end{bmatrix}, \quad B_i^{[s]} = \begin{bmatrix} \frac{-T}{C_{1s}} \\ 0 \\ 0 \end{bmatrix} \\ D_1^{[1]} &= \begin{bmatrix} 0.01 \\ 0.02 \\ -0.01 \end{bmatrix}, \quad E_1^{[1]} = \begin{bmatrix} 0.03 \\ 0.01 \\ 0.01 \end{bmatrix}, \quad L_1^{[1]} = 0.03 \\ D_2^{[1]} &= \begin{bmatrix} 0.01 \\ 0.01 \\ 0.03 \end{bmatrix}, \quad E_2^{[1]} = \begin{bmatrix} 0.01 \\ 0.01 \\ 0.02 \end{bmatrix}, \quad L_2^{[1]} = 0.01 \\ F_1^{[1]} &= 0.01, \quad F_2^{[1]} = 0.02, \quad F_1^{[2]} = 0.01, \quad F_2^{[2]} = 0.03 \\ D_1^{[2]} &= \begin{bmatrix} 0.02 \\ 0.01 \\ 0.01 \end{bmatrix}, \quad E_1^{[2]} = \begin{bmatrix} 0.01 \\ 0.02 \\ 0.01 \end{bmatrix}, \quad L_1^{[2]} = 0.02 \\ D_2^{[2]} &= \begin{bmatrix} 0.01 \\ 0.02 \\ 0.01 \end{bmatrix}, \quad E_2^{[2]} = \begin{bmatrix} 0.01 \\ 0.03 \\ 0.01 \end{bmatrix}, \quad L_2^{[2]} = 0.01 \end{aligned}$$

We choose $C_{11} = 0.764$, $C_{12} = 0.466$, $R = 1.637$, $C_2 = 8$, $L = 0.8$, $R_0 = 0.012$, $T = 0.1$, $\Lambda_a = -0.3$, $\Lambda_b = -0.01$, $\bar{V} = 1$, and $v_0 = 8$. The above is the whole process of discrete-time switching fuzzy modeling for the switching chua's circuit. By employing LMI algorithms, we obtain that the minimised feasible ξ is $\xi = 1.0042$ and $\xi = 1.0038$ in the full- and reduced-order residual system, respectively. Furthermore, $d(k)$ and $f(k)$ are selected as:

$$\begin{aligned} d(k) &= 0.8 \exp(-0.25k) \sin(0.4k), \quad k > 0 \\ f(k) &= 0.1 + 0.01 \sin(k), \quad 40 \leq k \leq 80 \end{aligned}$$

The full-order residual system simulation of Example 2 are not repeated here. Figs. 11-15 show the reduced-order residual system simulation results of Example 2. Figs. 11 and 12 show the states change of the dynamic residual system. The control input $u(k)$, residual signal $y_d(k)$, and evaluation function $F(y_d)$ are shown in Figs. 13-15, respectively. In the simulation results of full-order residual system, the maximum value of control input $u(k)$ in the process of dynamic response can reach 700(V), which is not desirable for switching Chua's circuit. However, Fig. 13 reflects the maximum value of the control input of the reduced-order residual system is only 6(V), which is more in line with the control requirements for the actual engineering system. Of course, this phenomenon is also shown in Example 1. As can be seen from Figs. 14 and 15, the change trend of the fault signal can be reflected by the residual function $y_d(k)$. When a fault signal appears, the residual evaluation function $F(y_d)$ has a large numerical mutation which is not in accordance with the normal

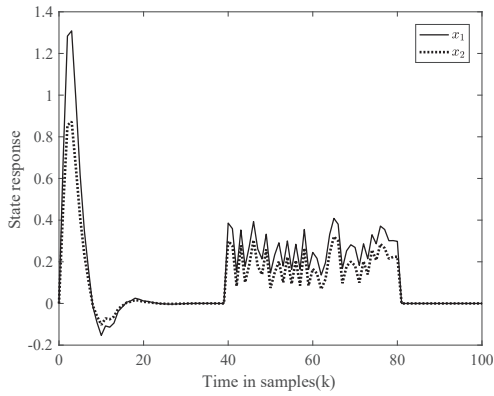


Fig. 11. The states of the original system in Example 2

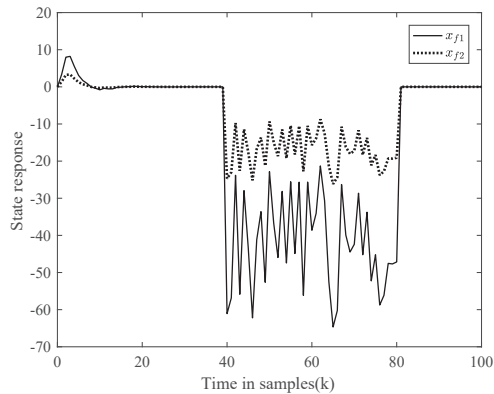


Fig. 12. The states of the control system in Example 2

condition. Finally, the appropriate threshold can be set to determine whether the fault occurs.

In general, the design of reduced-order fault detector and controller will not affect the fault detection and control of the original system. The experimental results show that the reduced-order fault detector and controller are more likely to be suitable for practical systems. In addition, compared with the full-order residual system, the reduced-order residual system can also maintain the \mathcal{H}_∞ performance close to the full-order dynamic residual system while reducing the computational complexity.

VI. Conclusion

This research addresses the problem of FRFDC design for discrete-time switching fuzzy systems. The average dwell time method is used to ensure that the dynamic residual system has mean-square exponential stability under any switching control law. Moreover, a segmented Lyapunov function is constructed to derive sufficient conditions that ensure that the corresponding residual system exponentially stabilizes with a balanced \mathcal{H}_∞ performance level (ξ, β) . Several linear matrix inequalities are derived using the linearization method, and the FRFDC parameters can be obtained using the mathematical solver

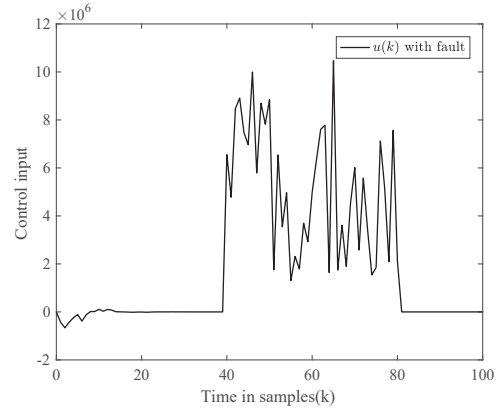


Fig. 13. Control input $u(k)$ in Example 2

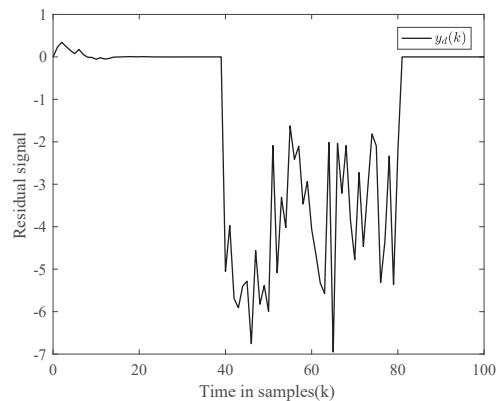


Fig. 14. Residual signal $y_d(k)$ in Example 2

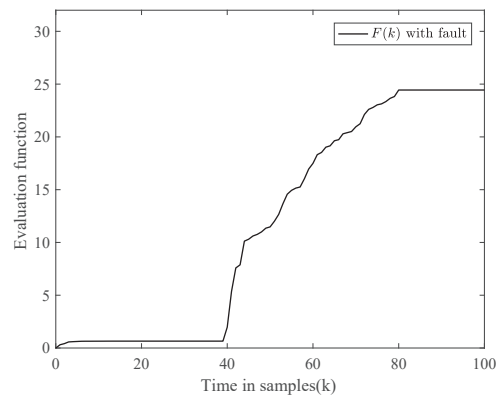


Fig. 15. Residual evaluation function $F(y_d)$ in Example 2

toolbox. Finally, two examples are considered to demonstrate the effectiveness of the proposed methods.

References

- [1] M. Hajiahmadi, B. De Schutter, and H. Hellendoorn, "Design of stabilizing switching laws for mixed switched affine systems," *IEEE Transactions on Automatic Control*, vol. 61, no. 6, pp. 1676-1681, 2016.
- [2] R. Guicherd, A. R. Mills, P. A. Trodden, and V. Kadiramanathan, "Simultaneous and sequential control design for discrete-time switched linear systems using semi-definite programming," *IEEE Control Systems Letters*, vol. 5, no. 4, pp. 1393-1398, 2021.
- [3] T. Sun, D. Zhou, Y. Zhu, and M. V. Basin, "Stability, l_2 -gain analysis, and parity space-based fault detection for discrete-time switched systems under dwell-time switching," *IEEE Transactions on Systems, Man, and Cybernetics: Systems*, vol. 50, no. 9, pp. 3358-3368, 2020.
- [4] T. Lee, Y. Tan, and I. Mareels, "Analyzing the stability of switched systems using common zeroing-output systems," *IEEE Transactions on Automatic Control*, vol. 62, no. 10, pp. 5138-5153, 2017.
- [5] M. T. Raza, A. Q. Khan, G. Mustafa, and M. Abid, "Design of fault detection and isolation filter for switched control systems under asynchronous switching," *IEEE Transactions on Control Systems Technology*, vol. 24, no. 1, pp. 13-23, 2016.
- [6] H. Qu, and J. Zhao, "Event-triggered H_∞ filtering for discrete-time switched systems under denial-of-service," *IEEE Transactions on Circuits and Systems I: Regular Papers*, vol. 68, no. 6, pp. 2604-2615, 2021.
- [7] X. Lin, and C. C. Chen, "Finite-time output feedback stabilization of planar switched systems with/without an output constraint," *Automatica*, vol. 131, 2021.
- [8] R. Precup, S. Preitl, E. M. Petriu, J. K. Tar, M. L. Tomescu, and C. Pozna, "Generic two-degree-of-freedom linear and fuzzy controllers for integral processes," *Journal of the Franklin Institute*, vol. 346, no. 10, pp. 980-1003, 2009.
- [9] H. K. Lam, "Stabilization of nonlinear systems using sampled-data output-feedback fuzzy controller based on polynomial-fuzzy-model-based control approach," *IEEE Transactions on Cybernetics*, vol. 42, no. 1, pp. 258-267, 2012.
- [10] Y. Tan, K. Wang, X. Su, F. Xue, and P. Shi, "Event-triggered fuzzy filtering for networked systems with application to sensor fault detection," *IEEE Transactions on Fuzzy Systems*, vol. 29, no. 6, pp. 1409-1422, 2021.
- [11] Z. Preitl, R. E. Precup, J. K. Tar, and M. Takács, "Use of multi-parametric quadratic programming in fuzzy control systems," *Acta Polytechnica Hungarica*, vol. 3, no. 9, pp. 29-43, 2006.
- [12] T. Chen, A. Babanin, A. Muḥammad, B. Chapron, and C. Chen, "Modified evolved bat algorithm of fuzzy optimal control for complex nonlinear systems," *Romanian Journal of Information Science and Technology*, vol. 23, no. T, pp. T28-T40, 2020.
- [13] R. E. Precup, S. Doboli, and S. Preitl, "Stability analysis and development of a class of fuzzy control systems," *Engineering Applications of Artificial Intelligence*, vol. 13, no. 3, pp. 237-247, 2000.
- [14] Y. Xue, B. C. Zheng, and X. Yu, "Robust sliding mode control for T-S fuzzy systems via quantized state feedback," *IEEE Transactions on Fuzzy Systems*, vol. 26, no. 4, pp. 2261-2272, 2018.
- [15] A. M. Whitbrook, U. Aickelin, and J. M. Garibaldi, "Idiotypic immune networks in mobile-robot control," *IEEE Transactions on Systems, Man, and Cybernetics*, vol. 37, no. 6, pp. 1581-1598, 2007.
- [16] J. Jean, and F. Lian, "Robust visual servo control of a mobile robot for object tracking using shape parameters," *IEEE Transactions on Control Systems Technology*, vol. 20, no. 6, pp. 1461-1472, 2012.
- [17] S. Mu, Z. Xiong, and Y. Tian, "Intelligent traffic control system based on cloud computing and big data mining," *IEEE Transactions on Industrial Informatics*, vol. 15, no. 12, pp. 6583-6592, 2019.
- [18] J. Dong, and G. Yang, "Dynamic output feedback control synthesis for continuous-time T-S fuzzy systems via a switched fuzzy control scheme," *IEEE Transactions on Cybernetics*, vol. 38, no. 4, pp. 1166-1175, 2008.
- [19] S. Sun, H. Zhang, Z. Qin, and R. Xi, "Delay-dependent H_∞ guaranteed cost control for uncertain switched T-S fuzzy systems with multiple interval time-varying delays," *IEEE Transactions on Fuzzy Systems*, vol. 29, no. 5, pp. 1065-1080, 2021.
- [20] S. Shi, Z. Fei, P. Shi, and C. K. Ahn, "Asynchronous filtering for discrete-time switched T-S fuzzy systems," *IEEE Transactions on Fuzzy Systems*, vol. 28, no. 8, pp. 1531-1541, 2020.
- [21] S. Sun, H. Zhang, C. Liu, and Y. Liu, "Dissipativity-based intermittent fault detection and tolerant control for multiple delayed uncertain switched fuzzy stochastic systems with unmeasurable premise variables," *IEEE Transactions on Cybernetics*, DOI: 10.1109/TCYB.2020.3041125.
- [22] Z. Wang, and J. Yuan, "Dissipativity-based composite antidisturbance control for T-S fuzzy switched stochastic nonlinear systems subjected to multisource disturbances," *IEEE Transactions on Fuzzy Systems*, vol. 29, no. 5, pp. 1226-1237, 2021.
- [23] H. Ohtake, K. Tanaka, and H. O. Wang, "Switching fuzzy controller design based on switching Lyapunov function for a class of nonlinear systems," *IEEE Transactions on Cybernetics*, vol. 36, no. 1, pp. 13-23, 2006.
- [24] H. K. Lam, and F. H. F. Leung, "Fuzzy combination of fuzzy and switching state-feedback controllers for nonlinear systems subject to parameter uncertainties," *IEEE Transactions on Cybernetics*, vol. 35, no. 2, pp. 269-281, 2005.
- [25] H. Sang, and J. Zhao, "Passivity and passification for switched T-S fuzzy systems with sampled-data implementation," *IEEE Transactions on Fuzzy Systems*, vol. 28, no. 7, pp. 1219-1229, 2020.
- [26] J. H. Zhang, J. J. Xia, J. M. Garibaldi, P. P. Groumos, and R. B. Wang, "Modeling and control of operator functional state in a unified framework of fuzzy inference petri nets," *Computer Methods and Programs in Biomedicine*, vol. 144, pp. 147-163, 2017.
- [27] X. Su, F. Xia, Y. Song, M. V. Basin, and L. Zhao, " \mathcal{L}_2 - \mathcal{L}_∞ output feedback controller design for fuzzy systems over switching parameters," *IEEE Transactions on Fuzzy Systems*, vol. 26, no. 6, pp. 3755-3769, 2018.
- [28] S. Priyanka, R. Sakthivel, S. Mohanapriya, F. Kong, and S. Saat, "Composite fault-tolerant and anti-disturbance control for switched fuzzy stochastic systems," *ISA Transactions*, <https://doi.org/10.1016/j.isatra.2021.06.022>, 2021.
- [29] T. Ince, S. Kiranyaz, L. Eren, M. Askar, and M. Gabbouj, "Real-time motor fault detection by 1-D convolutional neural networks," *IEEE Transactions on Industrial Electronics*, vol. 63, no. 11, pp. 7067-7075, 2016.
- [30] L. Wu, and D. W. C. Ho, "Fuzzy filter design for Itô stochastic systems with application to sensor fault detection," *IEEE Transactions on Fuzzy Systems*, vol. 17, no. 1, pp. 233-242, 2009.
- [31] M. R. Davoodi, K. Khorasani, H. A. Talebi, and H. R. Momeni, "Distributed fault detection and isolation filter design for a network of heterogeneous multiagent systems," *IEEE Transactions on Control Systems Technology*, vol. 22, no. 3, pp. 1061-1069, 2014.
- [32] S. Gautam, P. K. Tamboli, V. H. Patankar, K. Roy, and S. P. Duttgupta, "Sensors incipient fault detection and isolation using kalman filter and Kullback-Leibler divergence," *IEEE Transactions on Nuclear Science*, vol. 66, no. 5, pp. 728-794, 2019.
- [33] B. Pourbabae, N. Meskin, and K. Khorasani, "Sensor fault detection, isolation, and identification using multiple-model-based hybrid kalman filter for gas turbine engines," *IEEE Transactions on Control Systems Technology*, vol. 24, no. 4, pp. 1184-1200, 2016.
- [34] G. H. B. Foo, X. Zhang, and D. M. Vilathgamuwa, "A sensor fault detection and isolation method in interior permanent magnet synchronous motor drives based on an extended kalman filter," *IEEE Transactions on Industrial Electronics*, vol. 60, no. 8, pp. 3485-3495, 2013.
- [35] A. Chibani, M. Chadli, P. Shi, and N. B. Braiek, "Fuzzy fault detection filter design for T-S fuzzy systems in the finite-frequency domain," *IEEE Transactions on Fuzzy Systems*, vol. 25, no. 5, pp. 1051-2061, 2017.
- [36] D. Wang, W. Wang, and P. Shi, "Robust fault detection for switched linear systems with state delays," *IEEE Transactions on Cybernetics*, vol. 39, no. 3, pp. 800-805, 2009.
- [37] X. Su, X. Liu, Y. Song, H. K. Lam, and L. Wang, "Reduced-order model approximation of fuzzy switched systems with pre-

specified performance,” *Information Sciences*, vol. 370-371, pp. 538-550, 2016.

- [38] Y. Zeng, H. K. Lam, and L. Wu, “Hankel-norm-based model reduction for stochastic discrete-time nonlinear systems in interval type-2 T-S fuzzy framework,” *IEEE Transactions on Cybernetics*, vol. 51, no. 10, pp. 4934-4943, 2021.
- [39] X. Su, L. Wu, P. Shi, and C. L. P. Chen, “Model approximation for fuzzy switched systems with stochastic perturbation,” *IEEE Transactions on Fuzzy Systems*, vol. 23, no. 5, pp. 1458-1473, 2015.
- [40] L. Tang, and J. Zhao, “Switched threshold-based fault detection for switched nonlinear systems with its application to Chua’s circuit system,” *IEEE Transactions on Circuits and Systems*, vol. 66, no. 2, pp. 733-741, 2018.



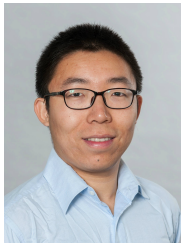
Yaoyao Tan received the B.E. degree in Automation from Wuhan Institute Of Technology, Hubei, China, in 2017, and is currently working towards the Ph.D. degree with the College of Automation, Chongqing University.

Her research interests include fuzzy control, fault detection/fault-tolerant control, and robot control.



Xiaojie Su received the PhD degree in Control Theory and Control Engineering from Harbin Institute of Technology, China in 2013. He is currently a professor and the associate dean with the College of Automation, Chongqing University, Chongqing, China. He has published 2 research monographs and more than 50 research papers in international referred journals.

His current research interests include intelligent control systems, advanced control, and unmanned system control. He currently serves as an Associate Editor for a number of journals, including *IEEE Systems Journal*, *IEEE Control Systems Letters*, *Information Sciences*, and *Signal Processing*. He is also an Associate Editor for the Conference Editorial Board, *IEEE Control Systems Society*. He was named to the 2017, 2018 and 2019 Highly Cited Researchers list, Clarivate Analytics.



Zhenshan Bing received his doctorate degree in Computer Science from the Technical University of Munich, Germany, in 2019. He received his B.S degree in Mechanical Design Manufacturing and Automation from Harbin Institute of Technology, China, in 2013, and his M.Eng degree in Mechanical Engineering in 2015, at the same university. Dr. Bing is currently a postdoctoral researcher with Informatics 6, Technical University of Munich, Munich, Germany. His research investigates

the snake-like robot which is controlled by artificial neural networks and its related applications.



Xiaokui Yang received the M.E. degree in Materials Science from Southwest University, Chongqing, China, in 2010, and is currently working towards the D.Eng. degree with the College of Automation, Chongqing University.

His research mainly focuses on the basic theory and scientific research on natural environment test and evaluation of products, including intelligent monitoring, control and comprehensive evaluation.



Alois Knoll (Senior Member) received his diploma (M.Sc.) degree in Electrical/Communications Engineering from the University of Stuttgart, Germany, in 1985 and his Ph.D. (summa cum laude) in Computer Science from Technical University of Berlin, Germany, in 1988. He served on the faculty of the Computer Science department at TU Berlin until 1993. He joined the University of Bielefeld, Germany as a full professor and served as the director of the

Technical Informatics research group until 2001, he has been a professor at the Department of Informatics, Technical University of Munich (TUM), Germany. He was also on the board of directors of the Central Institute of Medical Technology at TUM (IMETUM). From 2004 to 2006, he was Executive Director of the Institute of Computer Science at TUM. Between 2007 and 2009, he was a member of the EU’s highest advisory board on information technology, ISTAG, the Information Society Technology Advisory Group, and a member of its subgroup on Future and Emerging Technologies (FET). In this capacity, he was actively involved in developing the concept of the EU’s FET Flagship projects. His research interests include cognitive, medical and sensor-based robotics, multi-agent systems, data fusion, adaptive systems, multimedia information retrieval, model-driven development of embedded systems with applications to automotive software and electric transportation, as well as simulation systems for robotics and traffic.